

## Nonideal mixing in multicomponent lipid/detergent systems

This article has been downloaded from IOPscience. Please scroll down to see the full text article.

2006 J. Phys.: Condens. Matter 18 S1125

(<http://iopscience.iop.org/0953-8984/18/28/S02>)

View [the table of contents for this issue](#), or go to the [journal homepage](#) for more

Download details:

IP Address: 129.252.86.83

The article was downloaded on 28/05/2010 at 12:19

Please note that [terms and conditions apply](#).

# Nonideal mixing in multicomponent lipid/detergent systems

Alekos Tsamaloukas, Halina Szadkowska and Heiko Heerklotz

Biozentrum of the University of Basel, Division of Biophysical Chemistry, Klingelbergstrasse 70, CH-4056 Basel, Switzerland

E-mail: [aleko@oxphos.de](mailto:aleko@oxphos.de)

Received 15 November 2005, in final form 7 February 2006

Published 28 June 2006

Online at [stacks.iop.org/JPhysCM/18/S1125](http://stacks.iop.org/JPhysCM/18/S1125)

## Abstract

A detailed understanding of the mixing properties of membranes to which detergents are added is mandatory for improving the application and interpretation of detergent based protein or lipid extraction assays. For Triton X-100 (TX-100), a nonionic detergent frequently used in the process of solubilizing and purifying membrane proteins and lipids, we present here a detailed study of the mixing properties of binary and ternary lipid mixtures by means of high-sensitivity isothermal titration calorimetry (ITC). To this end the partitioning thermodynamics of TX-100 molecules from the aqueous phase to lipid bilayers composed of various mixtures of 1-palmitoyl-2-oleoyl-*sn*-glycero-3-phosphocholine (POPC), egg-sphingomyelin (SM), and cholesterol (cho) are characterized. Composition-dependent partition coefficients  $K$  are analysed within the frame of a thermodynamic model developed to describe nonideal mixing in multicomponent lipid/detergent systems. The results imply that POPC, fluid SM, and TX-100 mix almost ideally (nonideality parameters  $|\rho_{\alpha/\beta}| < RT$ ). However, favourable SM/cho ( $\rho_{SM/cho} \leq -6RT$ ) and unfavourable PC/cho interactions ( $\rho_{PC/cho} = 2RT$ ) may under certain conditions cause POPC/TX-100-enriched domains to segregate from SM/cho-enriched ones. TX-100/cho contacts are unfavourable ( $\rho_{cho/TX} = 4RT$ ), so the system tends to avoid them. That means, addition of TX-100 promotes the separation of SM/cho-rich from PC/TX-100-rich domains. It appears that cho/detergent interactions are crucial governing the abundance and composition of detergent-resistant membrane patches.

## 1. Introduction

The use of detergents is common practice in membrane research to study integral membrane proteins and lipids [1–3]. Selective solubilization techniques, that extract certain lipids and proteins but leave others in unsolubilized membrane patches, have a great potential. First,

they allow one to optimize the isolation of a membrane component. Second, they may provide insight into preferential interactions between different membrane constituents, such as lipids and proteins, in the original membrane. More than 30 years ago Steck and co-workers demonstrated in two careful experimental studies [4, 5] that the application of different reagents to isolated human erythrocyte membranes (also termed ghost membranes) can be used to selectively solubilize different proteins from this membrane. In their studies they found a 'reciprocal solubilization profile': protein perturbants like sodium hydroxide and others extracted mainly polar (hydrophilic) polypeptides from the membrane. In contrast, nonionic detergents like Triton X-100 (TX-100) mainly solubilized glycerolipid and glycoprotein, while in parallel yielding sphingolipid/cholesterol-enriched aggregates containing other classes of proteins as unsolubilized residues. With great caution concerning their experimental findings these authors noted that it is however speculative 'whether these aggregates arise by demixing following detergent action or exist in some form in the original ghost'.

Over approximately the last ten years, a vast body of literature has evolved that is essentially based on the assumption that so-called lipid raft domains [6–9] can be isolated as detergent-resistant membrane (DRMs) patches. However, it should be taken into account that the action of a detergent on a membrane system may alter the membrane domains (see, e.g., [7, 10, 11] for a discussion of the DRM = raft hypothesis). Studies employing model membrane systems have clearly demonstrated the ability of TX-100 to promote the formation of domains [12, 13] in a previously homogenous membrane. Furthermore, only recently it was shown by van Rheenen *et al* [14] that detergent treatment leads to a clustering of the phospholipid phosphatidylinositol 4,5-bisphosphate (PIP<sub>2</sub>) *in vivo*.

The complexity of the issue as well as its great practical potential is illustrated by the finding that different detergents can give rise to compositionally different DRMs from the same membrane [15–17]. If lipid/detergent (and in turn protein/detergent) interactions and their effects on fractions upon selective solubilization can be understood in a quantitative manner it may eventually become possible to rationally predict the optimum detergent for a given protein of interest. As a step in this direction Keller *et al* [18] have recently established a simple thermodynamic model describing the selective solubilization of membrane domains. These calculations suggest that nonideal mixing effects are necessary to explain the induction of ordered domains by a detergent before the onset of membrane solubilization. However, to date very few experimental data dealing with nonideal mixing in membranes to which detergents are added have been published. There is a clear need for such data in order to extend the model further. Binary mixtures of detergent (D) and unsaturated PC were treated in [19–21] analogously to the model of regular solutions [22]. This model describes nonideal properties of mixtures as the product of the statistical abundance of mixed pair interactions and constant nonideality parameters,  $\rho$ . These studies yielded typical values of  $\rho_{PC/D} \sim -0.7RT$ , suggesting a slightly favourable free energy of lipid/detergent mixing (compared to demixing) within a membrane.

A key for a better understanding of selective solubilization is detergent/cholesterol interactions, but these cannot be studied in binary systems because pure cholesterol forms no membranes. Here we overcome this problem by establishing a formalism suitable for deriving the nonideality parameters in ternary and quaternary systems. As such, taking as an example TX-100, that is used frequently in model system studies [23–26] as well as in the protein extraction procedure from biological membranes [27, 28], we study here in detail the mixing properties of TX-100 additive membranes by means of isothermal titration calorimetry (ITC). ITC can utilize three principal processes that allow quantifying the interaction of a solute with a membrane in terms of a partition coefficient,  $K$ , and a transfer enthalpy,  $\Delta H$ . Injection of membrane vesicles into a solution induces the uptake of solute into the membrane. Dilution of

solute-containing vesicles into an excess of buffer induces its release. The finding of a solute concentration in the calorimeter cell that causes neither uptake nor release [29] upon injection of solute-containing vesicles allows for a calculation of  $K$  as well (Rowe assay [30]).

The interaction parameters we collect from the modelling of our data provide a quantitative basis for the ability of a detergent to alter or induce domains in a membrane. Of course, great care must be taken when discussing the outcome of biochemical protocols in terms of fundamental physical parameters established in model systems. Nevertheless, biophysical model studies are valuable for recognizing problems, designing experiments, and understanding results obtained *in vivo*.

## 2. Materials and methods

### 2.1. Substances and sample preparation

The lipids 1-palmitoyl-2-oleoyl-*sn*-glycero-3-phosphocholine (POPC) and egg-sphingomyelin (eSM) were purchased from Avanti Polar Lipids, Alabaster, AL. Cholesterol (cho) and polyethylene glycol tert-octylphenyl ether (Triton X-100, TX-100) were from Fluka, Buchs, Switzerland. Mixtures of POPC and cho were prepared by addition of cho to the dry lipid powder, resuspension in chloroform/methanol, and consecutive drying under a gentle stream of nitrogen. Similarly, mixtures of POPC and eSM were prepared by adding appropriate amounts of eSM to the dry POPC lipid powder. All samples were held under vacuum for at least 12 h for further drying. The composition of the samples was checked by weighing the dry material before and after an addition. The dry lipid mixtures used for the uptake assays were suspended in 100 mM NaCl, 10 mM Tris buffer at pH 7.4 by gentle vortexing to reach a lipid concentration of 15 mM, i.e.,  $c_{PC} = 15$  mM for cho- and  $c_{PC} + c_{SM} = 15$  mM for SM-containing mixtures. In case of the samples used in the release as well as in the Rowe assay [30], the dry lipid film was suspended in a 1.5 mM TX-100 stock solution (or 0.25, 2.5, and 4 mM for experiments with pure POPC vesicles) to yield a lipid concentration (as defined above) of 15 mM. The values for the mole fraction of bound TX-100 in the membrane,  $X_{TX}^b$ , thus achieved are calculated afterwards based on the results obtained for the respective partition coefficient. After five consecutive freeze–thaw cycles, large unilamellar vesicles (LUVs) were prepared by ten extrusion runs through two stacked Nuclepore polycarbonate filters with a pore diameter of approximately 100 nm in a Lipex extruder (Northern Lipids Inc., Vancouver, Canada). Extrusion was performed at 50 °C for samples containing eSM due to its chain melting temperature of  $T_m \sim 39$  °C [13] and at room temperature for those containing POPC and cho.

### 2.2. ITC and DSC measurements

Isothermal titration calorimetry (ITC) experiments were performed on a VP ITC calorimeter from MicroCal, Inc. (Northampton, MA) [31, 32]. A total of 300  $\mu$ l of lipid suspension was injected in aliquots of a few  $\mu$ l (typical injection protocol:  $1 \times 1$ ,  $3 \times 5$ , and  $28 \times 10$   $\mu$ l) into a 1.4 ml cell containing either a TX-100 solution at concentration  $c_{TX}^{ini} = 50$ –150  $\mu$ M (uptake assay) or buffer (release assay) [29]. All partitioning experiments were conducted at 37 °C (see below for explanation). Data are displayed as normalized heats,  $Q_{obs}(c_L)$ , with normalization to the total number of moles of material (including cho) injected. Blank experiments, i.e., titration of lipid vesicles into buffer, showed small and constant heats of dilution, so instead of subtracting the  $Q_{obs}(c_L)$ -values obtained in these experiments, a constant heat of dilution is introduced as a third parameter into the model outlined below. In addition to uptake and release

experiments we have applied the Rowe protocol [30] as another independent way to determine the partition coefficient and enthalpy. Here the same LUVs as used in the release assay are titrated into solutions of different TX-100 concentration,  $c_{\text{TX}}^{\text{cell}}$ , loaded into the cell. The heat released or consumed upon the first 10  $\mu\text{l}$  injection (the first 1  $\mu\text{l}$  injection is not considered in the data evaluation) is plotted as a function of  $c_{\text{TX}}^{\text{cell}}$ . From the intercept with the  $c_{\text{TX}}^{\text{cell}}$ -axis (the total TX-100 concentration in the cell matches the free detergent concentration in the syringe) the partition coefficient can be calculated and the enthalpy is available from the slope of the curve (see the supporting information for details).

The differential scanning calorimetry (DSC) measurements were performed on a VP DSC calorimeter from MicroCal, Inc. (Northampton, MA) [33]. The sample cell of 0.5 ml was filled with a suspension of LUVs composed of mixtures of POPC and eSM with or without the above-mentioned TX-100 content in the membrane at a lipid concentration of 15 mM. For each sample a series of five consecutive scans with scan rates of 60, 30 and 10  $\text{K h}^{-1}$  was performed and the instrument was operated in the high-gain mode. All traces shown were corrected by the results obtained in blank experiments, i.e., scans where both calorimeter cells are filled with buffer. Data are presented as apparent isobaric heat capacity  $c_p$  as a function of temperature  $T$  normalized to the SM concentration in the membrane.

### 2.3. Data analysis and curve fitting

Analysis of the raw ITC traces was performed using Origin for ITC provided with the instrument and the DSC traces were correspondingly analysed using Origin for DSC. The normalized differential heats obtained from an integration of the power peaks resulting after each injection in an ITC experiment were exported to a Microsoft Excel spreadsheet and analysed therein similarly to what is detailed in [34]. For each SM- and cho-content in the membrane one release experiment was fitted globally against one uptake experiment. This procedure was repeated with (usually five) uptake experiments recorded at different  $c_{\text{TX}}^{\text{ini}}$  as specified above. The partition coefficients and molar transfer enthalpies listed are accordingly mean values with estimated maximal errors of  $\delta(K) = 15\%$ , and  $\Delta(\Delta H) = \pm 2 \text{ kJ mol}^{-1}$ , respectively.

## 3. Theory

### 3.1. Partitioning models

The partitioning of water-soluble substances into membranes (or their release from them) is described by different models [35]. Here we will use a model defined via

$$X_{\text{TX}}^{\text{b}} \equiv \frac{c_{\text{TX}}^{\text{b}}}{c_{\text{L}} + c_{\text{TX}}^{\text{b}}} = K c_{\text{TX}}^{\text{w}}, \quad (1)$$

where the concentration of membrane-bound TX-100,  $c_{\text{TX}}^{\text{b}}$ , is related to the amount of aqueous TX-100,  $c_{\text{TX}}^{\text{w}}$ , via the partition coefficient  $K$ . The total concentration of lipid (PC + cho, and PC + SM, respectively) quantified by the term  $c_{\text{L}}$  is assumed to be exclusively in the bilayer state, i.e., the aqueous concentration of lipid is assumed to be zero. We have omitted the constant factor  $c_{\text{w}} = 55.5 \text{ M}$  in (1) describing the concentration of water in a dilute aqueous solution resulting from the general definition of the mole fraction partition coefficient:  $K_X \equiv X_{\text{TX}}^{\text{b}}/X_{\text{TX}}^{\text{w}}$ . Therefore the partition coefficients listed have the dimension  $[K] = \text{mM}^{-1}$ . For small concentrations of bound detergent, i.e.,  $c_{\text{TX}}^{\text{b}} \ll c_{\text{L}}$ , the partition coefficient  $K$  defined by (1) approaches the mole-ratio partition coefficient defined as  $K \equiv c_{\text{TX}}^{\text{b}}/(c_{\text{L}}c_{\text{TX}}^{\text{w}})$  [35].

The mass conservation principle prescribes for the total TX-100 concentration within the calorimeter cell:  $c_{\text{TX}}^{\text{tot}} = c_{\text{TX}}^{\text{w}} + c_{\text{TX}}^{\text{b}}$ . Insertion into (1) yields a second-order polynomial in  $c_{\text{TX}}^{\text{b}}$ . The heat released or consumed upon an injection in an ITC experiment is linearly related to a change in the amount of bound detergent,  $\Delta c_{\text{TX}}^{\text{b}}$ , multiplied by the corresponding transfer enthalpy,  $\Delta H$ . Normalizing the heats of each injection with respect to the amount of lipid injected into the cell during this particular injection, one obtains normalized differential heats,  $Q_{\text{obs}}(c_{\text{L}})$ . These can be modelled according to the general expression (see [34] for further details)

$$Q_{\text{obs}}(c_{\text{L}}) = \frac{\Delta c_{\text{TX}}^{\text{b}}}{\Delta c_{\text{L}}} \Delta H + Q_{\text{dil}}, \quad (2)$$

where the term  $Q_{\text{dil}}$  denotes a small (usually less than 5% of  $\Delta H$ ), constant heat of dilution arising in any ITC experiment from effects other than partitioning or specific binding. The three-parameter model as detailed in (2) is based on the assumption that both the partition coefficient and enthalpy are constant during the course of an experiment. This need not be fulfilled in the most general situation; see for instance [19] and [21] for the case of a composition-dependent partition coefficient in binary mixtures. An extension to the case studied here, i.e., ternary mixtures, is given below.

### 3.2. Composition-dependent $K$ for a ternary mixture

We consider a lipid bilayer composed of POPC (the host fluid phase lipid), a second lipid denoted  $L_1$  (either SM or cho), and study the uptake/release of TX-100 by this system. The following equation for  $K$  as a function of membrane-bound TX-100,  $X_{\text{TX}}^{\text{b}}$ , can be derived (see the appendix for further details):

$$K(X_{\text{TX}}^{\text{b}}, \zeta_{\text{L}}) = K_{\text{PC}}(X_{\text{TX}}^{\text{b}}) \exp \left\{ -\frac{(1 - X_{\text{TX}}^{\text{b}})^2 \zeta_{\text{L}}}{RT(1 + \zeta_{\text{L}})} \left[ \rho_{\text{L}_1/\text{TX}} - \rho_{\text{PC}/\text{TX}} - \frac{\rho_{\text{PC}/\text{L}_1}}{1 + \zeta_{\text{L}}} \right] \right\}, \quad (3)$$

where  $\zeta_{\text{L}} = X_{\text{L}_1}/X_{\text{PC}} = n_{\text{L}_1}/n_{\text{PC}}$  denotes the mole ratio of the two lipids in the membrane, and  $K_{\text{PC}}(X_{\text{TX}}^{\text{b}})$  stands for the partition coefficient of TX-100 into a POPC membrane. The nonideality parameters (given as multiples of  $RT$ ,  $R$  being the universal gas constant and  $T$  the absolute temperature) for pairwise interactions are denoted by  $\rho_{\alpha/\beta}$  and are in general temperature dependent. They have the general form [22]

$$\rho_{\alpha/\beta} = \frac{N_{\text{A}}}{RT} z \left( \epsilon_{\alpha/\beta} - \frac{\epsilon_{\alpha/\alpha} + \epsilon_{\beta/\beta}}{2} \right), \quad (\alpha, \beta) \hat{=} \text{PC, L}_1, \text{TX}, \quad (4)$$

where, for example,  $\epsilon_{\alpha/\beta}$  denotes the energy of interaction of component  $\alpha$  with component  $\beta$  (in kJ),  $N_{\text{A}}$  is Avogadro's number, and  $z$  a coordination number (the number of lipid or detergent nearest neighbours).

In principle it is possible to insert (3) via the  $K$ -dependent value of  $c_{\text{TX}}^{\text{b}}$  into the model function (2) used to fit the ITC traces (solving (1) under the above-mentioned constraint for  $c_{\text{TX}}^{\text{tot}}$  yields a functional relation:  $c_{\text{TX}}^{\text{b}} = f(K, c_{\text{L}}, c_{\text{TX}}^{\text{tot}})$ ). However, this remains an implicit equation since the partition coefficient  $K$  depends on  $c_{\text{TX}}^{\text{b}}$  via (3) [21]. The differentiation with respect to  $c_{\text{L}}$  necessary in (2) can in principle be carried out using standard procedures for differentiating implicit functions [36] as performed for example in [21]. Following similar reasoning as put forward in [34] we have decided to refrain from fitting the data with a composition-dependent  $K$  and to afterwards analyse the trends observed in a series of experiments at different concentrations according to (3).

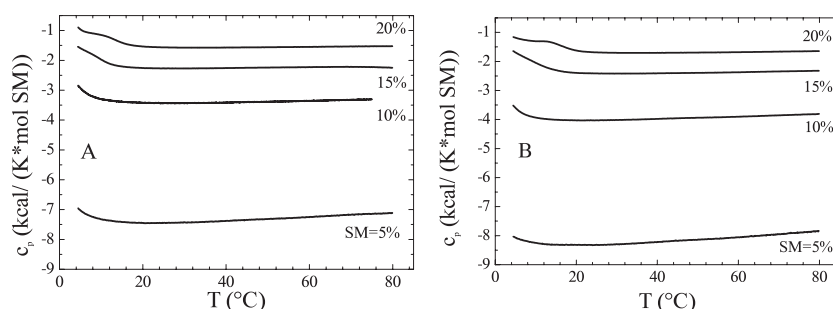


**Figure 1.** The apparent isobaric heat capacity  $c_p$  for mixtures of POPC and eSM with the eSM mole fraction,  $X_{SM}$ , as depicted in the plot. Panel (A): experiments with 15 mM LUVs without TX-100 bound to the membrane, and panel (B) for samples including TX-100 with a mole fraction of bound detergent of  $X_{TX}^b \sim 0.08$ .

## 4. Results

### 4.1. DSC

To avoid dealing with a membrane consisting of two coexisting phases, we checked the thermotropic behaviour of the POPC/SM-mixtures by means of DSC prior to performing the ITC experiments. Representative results for the mixtures used in the uptake as well as those in the release protocols are shown in figure 1 recorded at a scan rate of  $30 \text{ K h}^{-1}$ . As suggested by pure POPC melting at  $T_m \sim -2^\circ\text{C}$  [37] and eSM melting at  $T_m \sim 39^\circ\text{C}$  [13], we observe predominantly the high-temperature flank of the chain melting peak of the investigated binary lipid mixtures. The temperature where the transition is completed increases with increasing SM-content. In the case of the sample with  $X_{SM} = 0.2$ , the shoulder shifts from  $T_s \sim 10^\circ\text{C}$  up to  $T_s \sim 14^\circ\text{C}$  upon TX-100 inclusion ( $X_{TX}^b \sim 0.08$  as calculated with the mean value of the partition coefficient  $K$  given below) in the membrane. DSC traces have virtually returned to the baseline at  $37^\circ\text{C}$ . Therefore we point out that possible detrimental effects of a chain melting transition on both thermodynamic parameters accessible by ITC, i.e., the partition coefficient  $K$  and transfer enthalpy  $\Delta H$ , can be ruled out for the samples studied here.

### 4.2. ITC

**4.2.1. POPC/TX-100 interaction.** Figure 2 shows representative raw ITC data as well as the global analysis of one uptake and release experiment with POPC vesicles at  $37^\circ\text{C}$ . For the release assay, LUVs were prepared in a 1.5 mM TX-100 solution. Based on the mean value for the partition coefficient as obtained in the global fits, this corresponds to a membrane with a mole fraction of bound TX-100 of  $X_{TX}^b \sim 0.08$ . For the uptake experiment, the literature value for POPC/TX-100 interaction from [13] was used to decide upon the  $c_{TX}^{ini}$ -value. This experiment was consequently conducted at  $c_{TX}^{ini} = 75 \mu\text{M}$  in order to achieve an initial TX-100 content in the membrane close to that of the release sample. Additionally figure 2 shows a compilation of raw data of several experiments of the Rowe protocol injecting the same vesicles as used for the release assays into solutions with different TX-100 concentration,  $c_{TX}^{cell}$ , loaded into the cell. In panel (E) of figure 2 the heats resulting from an integration of the power peaks displayed in (D) are plotted as a function of  $c_{TX}^{cell}$ . The intercept with the  $c_{TX}^{cell}$ -axis corresponds to the free TX-100 concentration present in the syringe and can be directly used to calculate  $K$ . Based on the partitioning models explained in section 3, the slope of the



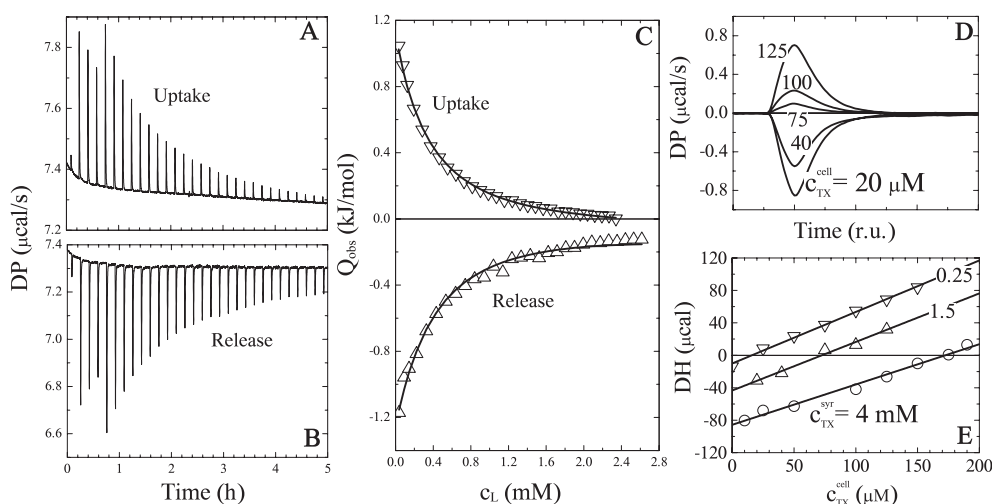


**Figure 2.** Experimental data of TX-100 interacting with POPC vesicles at  $T = 37^\circ\text{C}$ . Panels (A), (B): compensation heat power, DP, versus time for a typical injection protocol of  $1 \times 1$ ,  $3 \times 5$ , and  $26 \times 10 \mu\text{l}$ . (C): global analysis of the integrated, normalized heats of ITC uptake ( $\nabla$ ) and release ( $\Delta$ ) assay. Data fitting (solid lines) according to a  $X_{\text{TX}}^{\text{b}}$ -based partitioning model for a mole fraction of membrane-bound TX-100:  $X_{\text{TX}}^{\text{b}} \sim 0.08$ . Panel (D): raw experimental data of the Rowe protocol injecting  $10 \mu\text{l}$  POPC vesicles incubated with  $c_{\text{TX}}^{\text{syr}} = 1.5 \text{ mM}$  (total TX-100 concentration in the syringe) into solutions with different TX-100 concentration,  $c_{\text{TX}}^{\text{cell}}$ , loaded into the cell (all peaks are shifted such that the peak maximum coincides with time point  $t = 0$ ; therefore the  $x$ -axis is scaled in r.u.). Panel (E): plot of the heats resulting from an integration of the power peaks as shown in (D) for vesicles incubated with  $0.25 \text{ mM}$  ( $\nabla$ ),  $1.5 \text{ mM}$  ( $\Delta$ ), and  $4 \text{ mM}$  ( $\text{O}$ ) TX-100 solutions. Solid lines in (E) correspond to linear regressions to the data.

linear regressions shown in panel (E) of figure 2 can be used to determine the transfer enthalpy,  $\Delta H$  (see the supporting information for details). The dependence of the partition coefficient and transfer enthalpy on the mole fraction of membrane-bound TX-100,  $X_{\text{TX}}^{\text{b}}$ , is summarized in figure 3. Within the estimated accuracy of the two model parameters, the three different experimental assays utilized in this work yield consistent results. The resulting mean values are  $K = (1.2 \pm 0.2) \text{ mM}^{-1}$  for the partition coefficient, and  $\Delta H = (12 \pm 2) \text{ kJ mol}^{-1}$  for the transfer enthalpy, in agreement with the literature [13], respectively.

The small deviations that are observed in figure 3 do not allow us to speculate about asymmetric TX-100 incorporation into the membrane, slow detergent flip-flop, and other possible effects conceivable to explain deviations between uptake and release assay [29]. Given the restriction to small  $X_{\text{TX}}^{\text{b}}$  and the experimental uncertainty of  $K$ , the constancy of the mole fraction partition coefficient does not rule out that the system is equally well described by a constant mole-ratio partition coefficient (data not shown). Uptake experiments have to be carried out well below the critical micelle concentration (CMC) of TX-100 at  $37^\circ\text{C}$  ( $\text{CMC} \sim 230 \mu\text{M}$ , data not shown) but above  $c_{\text{TX}}^{\text{ini}} \sim 50 \mu\text{M}$  to achieve a satisfactory heat signal. Release experiments have to be performed well below the onset of membrane solubilization at  $(X_{\text{TX}}^{\text{b}})_{\text{sat}} = 0.29$  given in [13]. For membranes with  $X_{\text{TX}}^{\text{b}} \leq 0.05$  the heat signals obtained in a release assay are rather small, so we have instead applied the Rowe protocol [30] in the small- $X_{\text{TX}}^{\text{b}}$  regime.

**4.2.2. POPC/SM/TX-100 interaction.** Figure 4 shows the buffer/membrane partition coefficient for TX-100 and the corresponding molar transfer enthalpy as a function of the mole



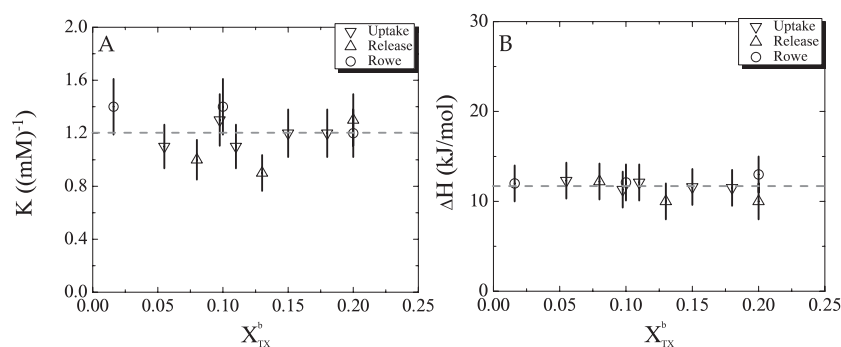


**Figure 3.** Plot of the buffer/membrane partition coefficient  $K$  (panel (A)) and partition enthalpy  $\Delta H$  (panel (B)) as a function of the mole fraction of bound TX-100 in the membrane,  $X_{TX}^b$ , determined at  $T = 37^\circ\text{C}$  for POPC LUVs. Results obtained with the three different assays are shown: fit parameters collected for uptake ( $\nabla$ ), release ( $\triangle$ ), and Rowe ( $\circ$ ) protocol. Dashed lines correspond to the mean values for  $K$  and  $\Delta H$  obtained from global fits to the uptake and release data with errors as given in the main text.

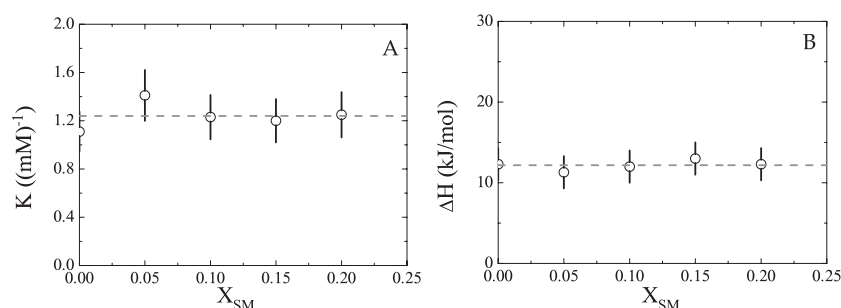


**Figure 4.** Panel (A): the buffer/membrane partition coefficient for TX-100,  $K$ , and the molar enthalpy change of transfer,  $\Delta H$  (panel (B)), as a function of the mole fraction of SM,  $X_{SM}$ , in the membrane measured at  $T = 37^\circ\text{C}$  with a mole fraction of bound TX-100,  $X_{TX}^b \sim 0.08$ . Data points correspond to the values obtained in global fits to uptake/release data (see text). Dashed lines correspond to the apparent mean value of  $K$  and  $\Delta H$ , respectively.

fraction of SM in the membrane,  $X_{SM}$ . The TX-100 content in the membrane was  $X_{TX}^b \sim 0.08$  as calculated with the value for the partition coefficient obtained from the global analysis of the data shown in figure 4. Within the assumed accuracy of the parameters, both parameters are independent of the SM mole fraction in the membrane. Mean values for the two parameters are  $K = (1.2 \pm 0.2) \text{ mM}^{-1}$  and  $\Delta H = (12 \pm 2) \text{ kJ mol}^{-1}$ , respectively.

**4.2.3. POPC/cho/TX-100 interaction.** In figure 5 the buffer/membrane partition coefficient for TX-100 and the corresponding molar transfer enthalpy are shown as a function of the mole fraction of cho in the membrane,  $X_{cho}$ . Based on the values collected for the partition coefficients for the various membranes investigated, the mole fraction of TX-100 in the membrane varies between  $X_{TX}^b \sim 0.06$  and  $X_{TX}^b \sim 0.10$ . While the partition coefficient decreases within the studied  $X_{cho}$ -interval from  $K = (1.2 \pm 0.2) \text{ mM}^{-1}$  at  $X_{cho} = 0$  to  $K = (0.5 \pm 0.1) \text{ mM}^{-1}$  at  $X_{cho} = 0.33$ , a concomitant increase ( $\sim 2.2\times$ ) of the transfer enthalpy is observed.

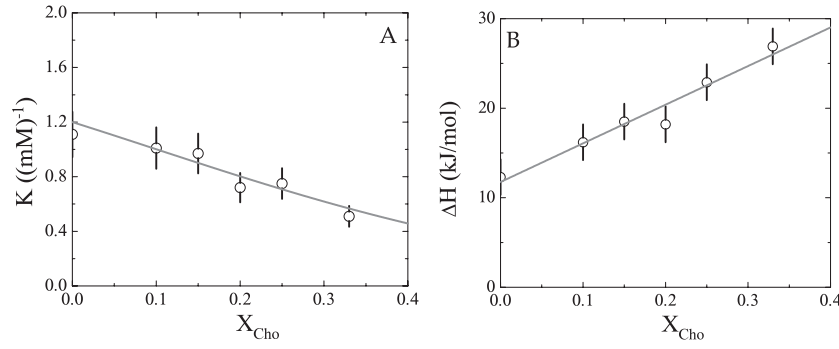


**Figure 5.** The buffer/membrane partition coefficient for TX-100,  $K$  (panel (A)), and the molar enthalpy change of transfer,  $\Delta H$  (panel (B)), as a function of the mole fraction of cho,  $X_{\text{cho}}$ , in the membrane measured at  $T = 37^\circ\text{C}$  with a mole fraction of bound TX-100,  $X_{\text{TX}}^{\text{b}} \sim 0.08$ . Data points correspond to the values obtained in global fits to uptake/release data (see text). Panel (B): one-parameter fit of  $K$  as a function of  $X_{\text{cho}}$  according to (5) using fixed values of  $K_{\text{PC}} = 1.2 \text{ mM}^{-1}$ ,  $\rho_{\text{PC}/\text{cho}} = 2RT$  [34],  $\rho_{\text{PC}/\text{TX}} = 0$ ,  $X_{\text{TX}}^{\text{b}} = 0.08$ , resulting in  $\rho_{\text{cho}/\text{TX}} = 4RT$ . The straight line in panel (B) is included as a guide to the eye and is not based on any model calculation.

## 5. Discussion

### 5.1. Pair interaction parameters for PC/SM/cho/TX-100

Our main goal is to provide a complete set of six nonideality parameters describing the mixing properties of PC/SM/cho membranes in the absence and presence of TX-100. We will therefore discuss the observed composition-dependent variations of  $K$  within the framework of the thermodynamic model outlined in section 3. The dependence of  $K$  on  $X_{\text{L}_1}$  will be investigated. Since the mole fractions of the species present in the membrane add up to unity, we can transform (3) into

$$K(X_{\text{L}_1}) = K_{\text{PC}}(X_{\text{TX}}^{\text{b}}) \exp \left\{ - \frac{(1 - X_{\text{TX}}^{\text{b}})(1 - X_{\text{TX}}^{\text{b}} - X_{\text{L}_1})X_{\text{L}_1}}{RT} \right. \\ \left. \times \left[ \frac{\rho_{\text{L}_1/\text{TX}} - \rho_{\text{PC}/\text{TX}}}{1 - X_{\text{TX}}^{\text{b}} - X_{\text{L}_1}} - \frac{\rho_{\text{PC}/\text{L}_1}}{1 - X_{\text{TX}}^{\text{b}}} \right] \right\}. \quad (5)$$

For the two ternary mixtures we will use  $X_{\text{TX}}^{\text{b}} = 0.08$  as the mole fraction of bound TX-100 present in our experiments to transform (5) into a simple, analytical function of one variable:  $X_{\text{L}_1}$ ; i.e., either  $X_{\text{SM}}$  or  $X_{\text{cho}}$ .

The thermodynamic parameters characterizing the system PC/SM/TX-100 show no significant deviations (within the studied  $X_{\text{SM}}$ -interval) from the values obtained for the binary mixture PC/TX-100. For a binary system, a constant  $K$  and/or  $\Delta H$  would immediately allow one to conclude that the two species mix in an ideal way. Because the first factor in the exponential function in (5) (the term outside the square brackets in (5)) does not vanish within reasonable intervals for both  $X_{\text{TX}}^{\text{b}}$ , i.e.,  $X_{\text{TX}}^{\text{b}} \in [0, 0.25]$ , and  $X_{\text{SM}}$ , i.e.,  $X_{\text{SM}} \in [0, 0.3]$  the term in square brackets must become zero. Using the estimate  $\rho_{\text{PC}/\text{TX}} = (0 \pm 1)RT$  describing the PC/TX-100 interaction that results from figure 3 we can conclude that  $\rho_{\text{PC}/\text{SM}}$  and  $\rho_{\text{SM}/\text{TX}}$  have to be zero as well. As such the addition of TX-100 to a membrane consisting of a mixture of a unsaturated lipid (PC) and a fluid, saturated lipid (SM, at the temperature of our experiments and within the  $X_{\text{SM}}$ -interval chosen) is very unlikely to induce the formation of domains.

The nonideal mixing behavior in the system PC/cho/TX-100 is apparent upon inspection of figure 5. We have modelled the dependence of  $K$  on  $X_{\text{cho}}$  with (5) using the following parameter assignments in a one-parameter fit:  $\rho_{\text{PC/cho}} = (2 \pm 1)RT$  as given in [34],  $\rho_{\text{PC/TX}} = (0 \pm 1)RT$  as resulting from this study, and  $K_{\text{PC}} = 1.2 \text{ mM}^{-1}$ . The resulting value for the nonideality parameter describing cho/TX-100 interaction is  $\rho_{\text{cho/TX}} = (4 \pm 1)RT$ . This result is insensitive to the value we assign to  $X_{\text{TX}}^{\text{b}}$ . For example, a variation of  $X_{\text{TX}}^{\text{b}}$  within the interval  $X_{\text{TX}}^{\text{b}} \in [0.06, 0.10]$  leads to values for  $\rho_{\text{cho/TX}}$  that stay well within the given error interval of this parameter. Furthermore, it is worth noting that in a two-parameter fit (the experimental data shown in figure 5 allow for at maximum two adjustable parameters) using both  $\rho_{\text{PC/TX}}$  and  $\rho_{\text{cho/TX}}$ , the former parameter stayed well within the interval given above. A slightly smaller positive detergent/cho nonideality parameter is implied by the data of Wenk *et al* in their studies of POPC/octyl- $\beta$ -D-glucopyranoside (OG) [38] and POPC/octyl- $\beta$ -thioglucopyranoside (OTG) [39] interaction. Their observation of constant mole ratio partition coefficients suggests small, negative PC/detergent nonideality parameters of  $\rho_{\text{PC/OG}} = \rho_{\text{PC/OTG}} \sim -0.7RT$ . Analysis of their data in the framework of our model yields for the detergent/cho nonideality parameters  $\rho_{\text{cho/OG}} = (3 \pm 1)RT$ , and  $\rho_{\text{cho/OTG}} = (3 \pm 1)RT$ , respectively. These experiments were conducted at  $T = 28^\circ\text{C}$ , so it can be expected that the nonideality parameters would be even smaller at  $T = 37^\circ\text{C}$ .

POPC/detergent interactions at room temperature were found to be only slightly nonideal with respect to the Gibbs free energy ( $\rho_{\text{PC/D}} \sim -0.7RT$ ), but this is often a result of a compensation of rather strongly unfavourable enthalpic and favourable entropic effects [20]. This behaviour can be explained with detergent-induced disordering of the membrane which perturbs intermolecular interactions ( $\Delta H > 0$ ) but increases motional and conformational freedom ( $\Delta S > 0$ ). This nonideality increases with increasing spontaneous curvature of the detergent and decreases with increasing temperature [20]. The lack of a detectable composition dependence of  $\Delta H$  found here (figure 3(B)) could be explained with the relatively high temperature and the very limited accessible range in  $X_{\text{TX}}^{\text{b}}$ . It is also intriguing that there seems to be no significant difference between the  $\Delta H$  of transfer into POPC and fluid SM, and the  $\Delta H$  of transfer into POPC alone. It appears that the specific behaviour of SM in domain-forming membranes requires the existence of an ordered (liquid ordered or gel) phase [25, 40] induced by low temperature, high SM-content and/or high cholesterol concentration.

## 5.2. The ‘canonical lipid raft mixture’

Let us consider the relationship between pair interactions studied in binary and ternary systems with the behaviour of a quaternary system. The partition coefficient  $K$  of TX-100 into POPC membranes is  $1.2 \text{ mM}^{-1}$ , addition of fluid SM has no effect on  $K$ , and addition of 33 mol% of cho reduces it to  $0.5 \text{ mM}^{-1}$ . However, a membrane containing an equimolar mixture of PC, SM, and cho (the so-called *canonical lipid raft mixture*) has an even lower  $K = (0.2 \pm 0.1) \text{ mM}^{-1}$  [13]. The quaternary mixture differs from the ternary ones (PC/cho/TX-100 and PC/SM/TX-100) by the additional existence of SM/cho contacts, some of which are broken by added TX-100 and replaced by TX/cho and TX/SM contacts. The fact that SM/cho interactions oppose TX-100 incorporation (reducing  $K$ ) implies that they must be favourable ( $\rho_{\text{SM/cho}} < 0$ ). That means, there is a tendency (opposed by the entropy of mixing) to form more than the random number of SM/cho contacts in a mixture. If such a tendency dominates the free energy of a system, the molecules may form superlattices [41, 42] or complexes [43, 44]. A quantitative estimate is possible using an expression for  $K$  in a homogeneously mixed, four-component system as given in the supporting information. Simulation of  $K$  on the basis of the parameters derived above and variable  $\rho_{\text{SM/cho}}$  reveals that a value of  $\rho_{\text{SM/cho}} = -(6 \pm 3)RT$

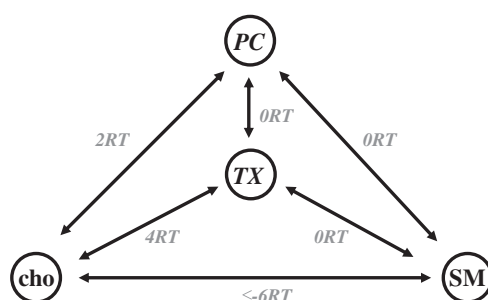


**Figure 6.** Free energy nonideality parameters  $\rho_{\alpha/\beta}$  at  $T = 37^\circ\text{C}$  describing the mixing properties in the quaternary mixture POPC/eSM/cho/TX-100. Errors for the  $\rho_{\alpha/\beta}$  determined for the two ternary mixtures (left-hand side and right-hand side triangle) in this study are of the order  $\pm 1RT$ . The value for  $\rho_{\text{SM}/\text{cho}}$  was estimated with the help of the literature value for the partition coefficient of TX-100 given in [13] (see text).

accounts for the experimental value of  $K = (0.2 \pm 0.1) \text{ mM}^{-1}$  assuming virtually random mixing.

For a membrane containing PC, SM, and cho, the parameters in figure 6 imply a tendency to demix into a PC-rich phase (thus reducing unfavourable PC/cho contacts) and a SM/cho-rich phase (to avoid replacing favourable SM/cho contacts by PC/SM and PC/cho contacts). Such a demixing is indeed occurring in the PC/SM/cho system at lower temperature [12]. It should be noted that the existence or induction of few residual ordered domains at  $37^\circ\text{C}$  would, for example, avoid some TX/cho contacts, so  $K$  into a hypothetical random mixture of PC/SM/cho would be even smaller than  $0.2 \text{ mM}^{-1}$ . Taking this into account, the determination of the nonideality parameter assuming random mixing yields an upper limit,  $\rho_{\text{SM}/\text{cho}} \leq -6RT$ .

### 5.3. Selective solubilization and detergent resistance

The nonideality parameters collected in figure 6 suggest that Triton added to a homogeneously mixed PC/SM/cho membrane has two unfavourable effects: it interacts unfavourably with cho and it interrupts favourable SM/cho contacts. Both these effects can be avoided (at the expense of mixing entropy) if TX-100 is (along with most PC) separated from much of the SM and cho into different domains. That means that, in the extreme case, addition of TX-100 could promote domain formation in a previously homogeneous membrane, as suggested experimentally [12]. If there are preexisting domains, added TX-100 would partition preferentially into PC-rich domains and tend to enhance the sorting of the lipids, as discussed in [18]. The fact that the local cho-content is reduced in the environment of TX-100 (rendering  $\Delta H$  smaller) and the Triton-induced transfer of cho from PC-rich into SM-rich domains (an accompanying, exothermic effect) might also explain why TX-100 partitioning into PC/SM/cho membranes (1:1:1, mole) at  $37^\circ\text{C}$  is less endothermic,  $\Delta H = 18 \text{ kJ mol}^{-1}$  [13], than into PC/cho (2:1, mole),  $\Delta H = 26 \text{ kJ mol}^{-1}$ . The above discussion implies that the nonideality parameter of a detergent interacting with cho,  $\rho_{\text{cho}/\text{D}}$ , may belong to the key parameters governing the abundance and composition of the detergent-resistant membrane fraction. The latter differ greatly between different detergents [16, 17]. For octyl glucoside (OG),  $\rho_{\text{cho}/\text{OG}}$  is most likely smaller than for TX-100 (see above), so the balance between the general disordering effect of a detergent and the specific, ordered domain-promoting effect [18] arising from  $\rho_{\text{cho}/\text{D}}$  is altered in favour of disorder and solubilization. Indeed, OG has been found to yield a smaller DRM fraction than TX-100 from Madin-

Darby canine kidney (MDCK) epithelial cells which was less enriched in cho and SM [15]. A detailed understanding of nonideal interactions of different detergents with different lipids may in the future allow for an optimization of selective solubilization procedures for different classes of membrane proteins. It will also shed light on the issue of what the selective solubilization of a protein along with certain lipids reveals about protein–lipid interactions *in vivo*.

### Acknowledgments

Financial support from the Swiss National Science Foundation (grant 31-67216.01) is gratefully acknowledged. We thank Sandro Keller (FMP Berlin) for important comments on this manuscript.

### Appendix. Derivation of equation (3)

For a general ternary mixture we can write for the mole fractions in the membrane

$$X_{\text{PC}} + X_{\text{L}_1} + X_{\text{TX}}^{\text{b}} = 1, \quad (\text{A.1})$$

and for the mole ratio of the two lipid components in the membrane

$$\zeta_{\text{L}} = \frac{X_{\text{L}_1}}{X_{\text{PC}}} = \frac{n_{\text{L}_1}}{n_{\text{PC}}}, \quad (\text{A.2})$$

which is, in contrast to the lipid mole fractions, conserved upon addition of TX-100. The expressions  $n_{\alpha}$  in (A.2) are in general used for the mole number of component  $\alpha$ .

The interaction terms in the molar excess free energy  $G_{\text{E}}$  (in  $\text{kJ mol}^{-1}$ ) are given by

$$G_{\text{E}} = \rho_{\text{PC/L}_1} X_{\text{PC}} X_{\text{L}_1} + \rho_{\text{PC/TX}} X_{\text{PC}} X_{\text{TX}}^{\text{b}} + \rho_{\text{L}_1/\text{TX}} X_{\text{L}_1} X_{\text{TX}}^{\text{b}}. \quad (\text{A.3})$$

Equation (A.3) is readily transformed with (A.1) and (A.2) into

$$G_{\text{E}} = \left( \frac{1 - X_{\text{TX}}^{\text{b}}}{1 + \zeta_{\text{L}}} \right) \left[ \rho_{\text{PC/L}_1} \zeta_{\text{L}} \left( \frac{1 - X_{\text{TX}}^{\text{b}}}{1 + \zeta_{\text{L}}} \right) + \rho_{\text{PC/TX}} X_{\text{TX}}^{\text{b}} + \rho_{\text{L}_1/\text{TX}} \zeta_{\text{L}} X_{\text{TX}}^{\text{b}} \right]. \quad (\text{A.4})$$

We can then write for a composition-dependent partition coefficient in case of nonideal mixing [19] (the constant factor  $c_{\text{W}}$  omitted in our definition of  $K$  in (1) has to be included now to render the argument of the logarithm dimensionless)

$$-RT \ln \left( K \left( X_{\text{TX}}^{\text{b}}, \zeta_{\text{L}} \right) \right) = \Delta\mu^0 + G_{\text{E}} + (1 - X_{\text{TX}}^{\text{b}}) \frac{\partial}{\partial X_{\text{TX}}^{\text{b}}} G_{\text{E}}, \quad (\text{A.5})$$

so that we obtain

$$K \left( X_{\text{TX}}^{\text{b}}, \zeta_{\text{L}} \right) = \exp \left( -\frac{\Delta\mu^0}{RT} \right) \exp \left\{ -\frac{(1 - X_{\text{TX}}^{\text{b}})^2}{RT(1 + \zeta_{\text{L}})} \left[ -\frac{\rho_{\text{PC/L}_1} \zeta_{\text{L}}}{1 + \zeta_{\text{L}}} + \rho_{\text{PC/TX}} + \rho_{\text{L}_1/\text{TX}} \zeta_{\text{L}} \right] \right\}. \quad (\text{A.6})$$

The term  $\Delta\mu^0 = \mu_{\text{TX}}^0(\text{bilayer}) - \mu_{\text{TX}}^0(\text{water})$  describes the change in standard chemical potential of TX-100 when partitioning from the aqueous phase into a hypothetical, pure TX-100 bilayer. Inserting  $\zeta_{\text{L}} = 0$  into (A.6), i.e., considering the case where TX-100 inserts into a POPC membrane, yields

$$K_{\text{PC}} \left( X_{\text{TX}}^{\text{b}} \right) = \exp \left( -\frac{\Delta\mu^0}{RT} \right) \exp \left( -\rho_{\text{PC/TX}} \frac{(1 - X_{\text{TX}}^{\text{b}})^2}{RT} \right), \quad (\text{A.7})$$

so that after simple rearrangements, (A.6) can be converted into (3).

## References

- [1] le Maire M, Kwee S, Andersen J P and Møller J V 1983 Mode of interaction of polyoxyethyleneglycol detergents with membrane proteins *Eur. J. Biochem.* **129** 525–32
- [2] le Maire M, Champeil P and Møller J V 2000 Interaction of membrane proteins and lipids with solubilizing detergents *Biochim. Biophys. Acta* **1508** 86–111
- [3] Garavito R M and Ferguson-Miller S 2001 Detergents as tools in membrane biochemistry *J. Biol. Chem.* **276** 32403–6
- [4] Steck T L and Yu J 1973 Selective solubilization of proteins from red blood cell membranes by protein perturbants *J. Supramol. Struct.* **1** 220–32
- [5] Yu J, Fischman D A and Steck T L 1973 Selective solubilization of proteins and phospholipids from red blood cell membranes by nonionic detergents *J. Supramol. Struct.* **1** 233–47
- [6] Simons K and Ikonen E 1997 Functional rafts in cell membranes *Nature* **387** 569–572
- [7] London E and Brown D A 2000 Insolubility of lipids in TX-100: physical origin and relationship to sphingolipid/cholesterol membrane domains (rafts) *Biochim. Biophys. Acta* **1508** 182–95
- [8] Simons K and Ehehalt R 2002 Cholesterol, lipid rafts, and disease *J. Clin. Invest.* **110** 597–603
- [9] Simons K and Vaz W L C 2004 Model systems, lipid rafts, and cell membranes *Annu. Rev. Biophys. Biomol. Struct.* **33** 269–96
- [10] Munro S 2003 Lipid rafts: elusive or illusive? *Cell* **115** 377–88
- [11] Lichtenberg D, Goñi F M and Heerklotz H 2005 Detergent-resistant membranes should not be identified with membrane rafts *Trends Biochem. Sci.* **30** 430–6
- [12] Heerklotz H 2002 Triton promotes domain formation in lipid raft mixtures *Biophys. J.* **83** 2693–701
- [13] Heerklotz H, Szadkowska H, Anderson T and Seelig J 2003 The sensitivity of lipid domains to small perturbations demonstrated by the effect of Triton *J. Mol. Biol.* **329** 793–9
- [14] van Rheenen J, Achame E M, Janssen H, Calafat J and Jalink K 2005 PIP<sub>2</sub> signaling in lipid domains: a critical re-evaluation *The EMBO J.* **24** 1664–73
- [15] Melkonian K A, Chu T, Tortorella L B and Brown D A 1995 Characterization of proteins in detergent-resistant membrane complexes from Madin–Darby canine kidney epithelial cells *Biochemistry* **34** 16161–70
- [16] Madore N, Smith K L, Graham C H, Jen A, Brady K, Hall S and Morris R 1999 Functionally different GPI proteins are organized in different domains on the neuronal surface *EMBO J.* **18** 6917–26
- [17] Schuck S, Honsho M, Ekroos K, Shevchenko A and Simons K 2003 Resistance of cell membranes to different detergents *Proc. Natl Acad. Sci. USA* **100** 5795–800
- [18] Keller S, Tsamaloukas A and Heerklotz H 2005 A quantitative model describing the selective solubilization of membrane domains *J. Am. Chem. Soc.* **127** 11469–76
- [19] Heerklotz H, Binder H, Lantzsch G and Klose G 1994 Membrane/water partition of oligo(ethylene oxide) dodecyl ethers and its relevance for solubilization *Biochim. Biophys. Acta* **1196** 114–22
- [20] Heerklotz H, Binder H, Lantzsch G, Klose G and Blume A 1997 Lipid/detergent interaction thermodynamics as a function of molecular shape *J. Phys. Chem. B* **101** 639–45
- [21] Keller M, Kerth A and Blume A 1997 Thermodynamics of interaction of octyl glucoside with phosphatidylcholine vesicles: partitioning and solubilization as studied by high sensitivity titration calorimetry *Biochim. Biophys. Acta* **1326** 178–92
- [22] Cevc G and Marsh D 1987 *Phospholipid Bilayers: Physical Principles and Models* 1st edn, vol 5 (New York: Wiley)
- [23] Goñi F M, Urbaneja M-A, Arrondo J L R, Alonso A, Durrani A A and Chapman D 1986 The interaction of phosphatidylcholine bilayers with Triton X-100 *Eur. J. Biochem.* **160** 659–65
- [24] Partearroyo M A, Urbaneja M A and Goñi F M 1992 Effective detergent/lipid ratios in the solubilization of phosphatidylcholine vesicles by Triton X-100 *FEBS Lett.* **302** 138–40
- [25] Nyholm T and Slotte J P 2001 Comparison of Triton X-100 penetration into phosphatidylcholine and sphingomyelin mono- and bilayers *Langmuir* **17** 4724–30
- [26] Schnitzer E, Lichtenberg D and Kozlov M M 2003 Temperature-dependence of the solubilization of dipalmitoylphosphatidylcholine (DPPC) by the non-ionic surfactant Triton X-100, kinetic and structural aspects *Chem. Phys. Lipids* **126** 55–76
- [27] Berthold D A, Babcock G T and Yocum C A 1981 A highly resolved, oxygen-evolving Photosystem II preparation from spinach thylakoid membranes *FEBS Lett.* **134** 231–4
- [28] Schiller H and Dau H 2000 Preparation protocols for high-activity Photosystem II membrane particles of green algae and higher plants, pH dependence of oxygen evolution and comparison of S<sub>2</sub>-state multiline signal by X-band EPR *J. Photochem. Photobiol. B* **55** 138–44
- [29] Heerklotz H 2004 Microcalorimetry of lipid membranes *J. Phys.: Condens. Matter* **16** 441–67

- [30] Zhang F and Rowe E S 1992 Titration calorimetric and differential scanning calorimetric studies of the interactions of *n*-butanol with several phases of dipalmitoylphosphatidylcholine *Biochemistry* **31** 2005–11
- [31] Wiseman T, Williston S, Brandts J F and Lin L N 1989 Rapid measurement of binding constants and heats of binding using a new titration calorimeter *Anal. Biochem.* **179** 131–7
- [32] Chellani M 1999 Isothermal titration calorimetry: biological applications *Am. Biotechnol. Lab.* **17** 14–8
- [33] Plotnikov V V, Brandts J M, Lin L N and Brandts J F 1997 A new ultrasensitive scanning calorimeter *Anal. Biochem.* **250** 237–44
- [34] Tsamaloukas A, Szadkowska H, Slotte J P and Heerklotz H 2005 Interactions of cholesterol with lipid membranes and cyclodextrin characterized by calorimetry *Biophys. J.* **89** 1109–19
- [35] Heerklotz H and Seelig J 2000 Titration calorimetry of surfactant-membrane partitioning and membrane solubilization *Biochim. Biophys. Acta* **1508** 69–85
- [36] Zachmann H G 1994 *Mathematik für Chemiker* 5th edn (Weinheim: VCH)
- [37] Koynova R and Caffrey M 1998 Phases and phase transitions of the phosphatidylcholines *Biochim. Biophys. Acta* **1376** 91–145
- [38] Wenk M R, Alt T, Seelig A and Seelig J 1997 Octyl- $\beta$ -D-glucopyranoside partitioning into lipid bilayers: thermodynamics of binding and structural changes of the bilayer *Biophys. J.* **72** 1719–31
- [39] Wenk M R and Seelig J 1997 Interaction of octyl- $\beta$ -thioglucopyranoside with lipid membranes *Biophys. J.* **73** 2565–74
- [40] Ollila F and Slotte J P 2002 Partitioning of Triton X-100, deoxycholate and C<sub>10</sub>EO<sub>8</sub> into bilayers composed of native and hydrogenated egg yolk sphingomyelin *Biochim. Biophys. Acta* **1564** 281–8
- [41] Huang J 2002 Exploration of molecular interactions in cholesterol superlattices: effect of multibody interactions *Biophys. J.* **83** 1014–25
- [42] Cannon B, Heath G, Huang J, Somerharju J A, Virtanen J A and Cheng K H 2003 Time-resolved fluorescence and Fourier transform infrared spectroscopic investigations of lateral packing defects and superlattice domains in compositionally uniform cholesterol/phosphatidylcholine bilayers *Biophys. J.* **84** 3777–91
- [43] Radhakrishnan A and McConnell H M 1999 Condensed complexes of cholesterol and phospholipids *Biophys. J.* **77** 1507–17
- [44] Radhakrishnan A, Anderson T G and McConnell H M 2000 Condensed complexes, rafts and the chemical activity of cholesterol in membranes *Proc. Natl Acad. Sci. USA* **97** 12422–7